

The evolution of the binary population in globular clusters: a full analytical computation

A. Sollima[★]

Istituto de Astrofísica de Canarias, C/Vía Lactea s/n, San Cristobal de La Laguna, Tenerife 38205-E, Spain

Accepted 2008 April 24. Received 2008 April 24; in original form 2008 February 20

ABSTRACT

I present a simplified analytical model that simulates the evolution of the binary population in a dynamically evolving globular cluster. A number of simulations have been run spanning a wide range in initial cluster and environmental conditions by taking into account the main mechanisms of formation and destruction of binary systems. Following this approach, I investigate the evolution of the fraction, the radial distribution, the distribution of mass ratios and periods of the binary population. According to these simulations, the fraction of surviving binaries appears to be dominated by the processes of binary ionization and evaporation. In particular, the frequency of binary systems changes by a factor of 1–5 depending on the initial conditions and on the assumed initial distribution of periods. The comparison with the existing estimates of binary fractions in Galactic globular clusters suggests that significant variations in the initial binary content could exist among the analysed globular cluster. This model has been also used to explain the observed discrepancy found between the most recent N -body and Monte Carlo simulations in the literature.

Key words: stellar dynamics – methods: analytical – binaries: general – globular clusters: general.

1 INTRODUCTION

The study of the evolution of binary stars both in the solar neighbourhood and in stellar clusters is one of the most interesting topics of stellar astrophysics. Binarity, under particular conditions, induces the onset of nuclear reactions leading to the formation of peculiar objects like novae and determines the fate of low-mass stars leading to supernova type Ia (SNIa) explosions. In collisional systems binaries provide the gravitational fuel that can delay and eventually stop and reverse the process of core collapse in globular clusters (see Hut et al. 1992a, and references therein). Furthermore, the evolution of binaries in star clusters can produce peculiar stellar objects of astrophysical interest like blue stragglers, cataclysmic variables, low-mass X-ray binaries, millisecond pulsars, etc. (see Bailyn 1995, and reference therein).

From an observational point of view, there is an extensive literature on the analysis of the main characteristics of the binary population of the Galactic field (Duquennoy & Mayor 1991; Halbwachs et al. 2003 and references therein). Conversely, the analysis of the binary population in star clusters is still limited to small samples of open clusters (Bica & Bonatto 2005) and to few globular clusters (Romani & Weinberg 1991; Bolte 1992; Yan & Mateo 1994; Yan & Cohen 1996; Yan & Reid 1996; Rubenstein & Bailyn

1997; Albrow et al. 2001; Bellazzini et al. 2002; Clark, Sandquist & Bolte 2004; Zhao & Bailyn 2005). More recently, Sollima et al. (2007) estimated the binary fraction in 13 low-density Galactic globular clusters. They found that the fractions of binary systems span a wide range comprising 10–50 per cent. This spread could be due either to differences in the primordial binary fractions or to a different evolution of the binary populations.

Theoretical studies addressed to the study of the evolution of the properties of the binary population in globular clusters are mainly based on two different approaches: (i) full N -body simulations and (ii) Monte Carlo simulations. The former follows the dynamical evolution of the stellar system assuming simplified treatments of single and binary star evolution (see Portegies Zwart et al. 2001; Shara & Hurley 2002; Hurley & Shara 2003; Hurley, Aarseth & Shara 2007; Trenti, Heggie & Hut 2007). This approach is extremely expensive computationally and has been often performed with unrealistically small numbers of binaries. The latter method uses a binary population synthesis code to evolve large numbers of stars and binaries by introducing a simple treatment of dynamics. In this type of approach it is often assumed that all the relevant parameters of the cluster (central density, velocity dispersion, mass, etc.) remain constant during the cluster evolution (see Hut, McMillan & Romani 1992b; Di Stefano & Rappaport 1994; Davies 1995; Davies & Benz 1995; Sigurdsson & Phinney 1995; Davies 1997; Portegies Zwart et al. 1997a; Portegies Zwart, Hut & Verbunt 1997b; Rasio, Pfahl & Rappaport 2000; Smith & Bonnell 2001; Ivanova et al.

[★]E-mail: asollima@iac.es

2005). The most recent works performed following these two different approaches led to apparently contradictory results: while Monte Carlo simulations (Ivanova et al. 2005) predict a strong depletion of the binary population in the cluster core, the N -body simulations performed by Hurley et al. (2007) show a progressive increase of the core binary fraction as a function of time.

In this paper I study the evolution of the binary population in a dynamically evolving globular cluster using a simplified analytical approach. Following this approach, I investigate the evolution of the fraction, the radial distribution, the distribution of mass ratios and periods of the binary population. A number of simulations have been run spanning a wide range in initial cluster and environmental conditions.

In Section 2 I describe in detail the code. In Section 3 I present the complete set of simulations and discuss the dependence of the results on the underlying assumptions. In Section 4 the predicted evolution of the binary fraction as a function of the initial cluster structural and environmental parameters is presented. Section 5 is devoted to the study of the radial distribution of binary systems. In Sections 6 and 7 the distribution of periods and mass ratios are investigated together with their dependence on the environmental conditions. A comparison with the most recent N -body and Monte Carlo simulations is performed in Section 8. In Section 9 the predictions of the code are compared with the estimates of binary fractions in globular clusters available in the literature. Finally, I discuss the obtained results in Section 10.

For clarity, I list below the notation used throughout the paper.

General:	
ρ_r	density at the distance r from the cluster centre
$\sigma_{v,r}$	velocity dispersion at the distance r
r_c	core radius
r_t	tidal radius
ξ	binary fraction
ξ_c	core binary fraction
ν	fraction of evaporating systems
t_0	cluster age
α	IMF power-law index
$\langle m \rangle$	average object mass (binaries + single stars)
N_{sys}	number of cluster objects (binaries + single stars)
M	cluster mass
M_c	cluster core mass
t_r	local relaxation time at the distance r
r_{rel}	relaxation radius
x	polytropic index
$f(v, r)$	distribution of velocities at the distance r
σ_X	cross-section of the process X
$v_{e,r}$	escape velocity at the distance r
G	Newton constant
$\log \Lambda$	Coulomb logarithm
Φ_r	potential at the distance r
ϵ_r	energy per unity of mass at the distance r
Binaries:	
m_1	mass of the primary star

m_2	mass of the secondary star
P	period
η	hardness parameter
E_b	binding energy
$N_b(m_1, m_2, \log P)$	number of binaries with parameters $m_1, m_2, \log P$
$n_{b,r}(m_1, m_2, \log P)$	number density of binaries with parameters $m_1, m_2, \log P$ at the distance r
$g(\log P)$	distribution of periods
q	mass ratio
Single stars:	
m_s	mass
$N_s(m_s)$	number of single stars with mass m_s
$n_{s,r}(m_s)$	number density of single stars with mass m_s at the distance r

2 METHOD

Each simulation is characterized by four initial parameters: the cluster central density ρ_0 , the central velocity dispersion $\sigma_{v,0}$, the initial binary fraction ξ and the rate of evaporating systems ν .

The code simulates the evolution of the number of binaries and single stars by taking into account the main processes of formation, destruction and evolution of binaries and single stars. In particular, the following processes have been considered:

- (i) tidal capture
- (ii) direct collisions
- (iii) exchanges
- (iv) collisional hardening
- (v) binaries ionization
- (vi) stellar evolution
- (vii) coalescence
- (viii) mass segregation
- (ix) evaporation

A detailed description of the analytical treatment of each of these processes is given in Sections 2.2–2.7. Moreover, during its evolution, the cluster dynamical parameters are assumed to evolve (see Section 2.8).

The binary population of the system has been divided in several groups according to the masses of the primary and secondary stars (m_1 and m_2), and to the period (P). Similarly, the population of single stars has been divided in groups of masses (m_s).

The evolution of each population of single and binary stars is calculated in layers of variable width located at different distances from the cluster centre.

At the beginning of the simulation, the density and the distribution of velocities of both single and binary stars is assumed to follow the radial behaviour of a monomass King profile, as expected for a non-relaxed stellar system. During this initial stage, the cluster is assumed to be a non-collisional system. Therefore, the only processes at work are those related to stellar evolution and evaporation.

After this initial stage, the evolution of the cluster and its binary population is followed in time-steps. For each time-step the adopted general procedure is schematically the following.

- (i) The code calculates the maximum radius in which the local relaxation time is smaller than the cluster age (*relaxation radius*; r_{rel}). The local relaxation time at the radius r has been calculated

using the relation

$$t_r = 0.34 \frac{\sigma_{v,r}^3}{G^2 \rho_r \langle m \rangle \log \Lambda} \quad (\text{Binney Tremaine 1987}) \quad (1)$$

with $\Lambda = 0.4 N_{\text{sys}}$.

(ii) The number of newly formed and destroyed binary systems have been calculated in all the layers located inside the *relaxation radius*. The number of binaries $N_b(m_1, m_2, \log P)$ and single stars $N_s(m_s)$ belonging to each group have been consequently updated.

(iii) A set of partially relaxed multimass King profiles has been calculated (see Appendix A). The density and velocity distribution of each subpopulation of binary and single stars have been assumed to follow a given profile according to their systemic masses.

(iv) The mass of the cluster has been calculated and the values of ρ_0 , $\sigma_{v,0}$ and W_0 have been updated (see Section 2.8).

Points (i)–(iv) have been repeated until the cluster reach an age of 13 Gyr. In the next subsection I will report the assumptions made in all the simulations presented in this paper.

2.1 Assumptions

The simulations have been performed assuming a time-step of $\Delta t = 0.1$ Gyr. This quantity has been chosen to be larger than the cluster crossing time, in order to ensure that all the stars of a given mass group can approach the radial distribution predicted by their own King profile, and short enough to avoid significant variations of the cluster structural parameters. During each time-step, the equivalent effect of the multiple interactions that occur for a binary population is calculated.

The width of the layers has been chosen to allow a higher resolution in the inner (i.e. more populated) regions of the cluster. I assumed $\Delta r = 0.1 r_c$ for $r < 5 r_c$, $\Delta r = r_c$ for $5 < r/r_c < 50$ and $\Delta r = 10 r_c$ for $r > 50 r_c$.

The cluster stars have been divided in mass bins of size $0.1 M_\odot$ in the mass range $0.1 < M/M_\odot < 5$. An additional bin formed by stars in the mass range $5 < M/M_\odot < 120$ has been considered. These massive stars have lifetimes shorter than the time-step of the simulation and are removed during the first stage of evolution (see Section 2). I adopted the initial mass function (IMF) by Kroupa (2002), which can be written as a broken power law $dN = m^\alpha dm$, with $\alpha = -1.3$ for $0.1 < M/M_\odot < 0.5$, and $\alpha = -2.3$ for $M > 0.5 M_\odot$.

The initial mass ratios and periods distributions of the binary population have been chosen in agreement with the results of Duquennoy & Mayor (1991). In particular, the initial mass ratio distribution has been derived by random associating stars belonging to different mass bins. I assumed a lognormal distribution of periods $g(\log P)$ centred at $\log P(d) = 4.8$ and with a dispersion $\sigma_{\log P} = 2.3$, where P is the period expressed in days. The corresponding semi-axes distribution of each group of binaries can be derived by considering the third Kepler's law

$$a = \left[\frac{G (m_1 + m_2) P^2}{4\pi^2} \right]^{1/3}.$$

The distribution of periods has been truncated assuming an upper limit¹ of $P = 10^7$ d in agreement with Sills et al. (2003). More-

over, a lower limit has been imposed by rejecting all the binaries whose major semi-axes (a) turn out to be lower than their limiting orbital distance (a_{min} ; see Section 2.6). The distribution of binary eccentricities has been assumed to follow a thermal distribution with probability density $p(e) = 2e$.

The mass–radius relation and the evolutionary time-scales of each mass group have been derived from the models by Pietrinferni et al. (2006) assuming a metal mass fraction $Z = 10^{-3}$.

In order to limit the number of free parameters, I assumed the King parameter W_0 as a linear combination of the central density and velocity dispersion

$$W_0 = \left[\log \left(\frac{\rho_0}{M_\odot \text{pc}^3} \right) - 2 \log \left(\frac{\sigma_{v,0}}{\text{km s}^{-1}} \right) \right] 1.921 + 2.934. \quad (2)$$

This relation has been derived empirically using the central densities and velocity dispersions reported by Djorgovski (1993) and the cluster concentrations by Trager, King & Djorgovski (1995). In the same way, the core radius r_c has been assumed to be linked to the above parameters in the following way:

$$r_c = \left(\frac{\sigma_{v,0}}{\text{km s}^{-1}} \right) \left(\frac{M_c}{10^{2.67} M_\odot} \right)^{-1/2} \text{ pc} \quad (\text{Bellazzini 1998}).$$

The dependence of the obtained results on the choice of some of these assumptions is investigated in Section 3.

2.2 Tidal capture

A mechanism proposed to form binary systems is based on the tidal capture of a companion induced by a close encounter between two single stars (Clark 1975). Indeed, when two colliding stars approach with a relative velocity and an impact parameter lower than given limits, they can form a bound system. The rate of binary systems formed through this mechanism has been evaluated using the cross-section σ_{tc} provided by Kim & Lee (1999). I considered the collisions between two non-degenerate stars with a polytropic index $x = 1.5$ (see their equation 6). In a time interval Δt , the number of tidal captured binaries having primary and secondary masses m_1 and m_2 and period P turns out to be

$$\Delta N_b(m_1, m_2, \log P) = \int_0^{r_{\text{rel}}} \frac{dN_{b,tc}}{dV} d^3 r,$$

where

$$\frac{dN_{b,tc}}{dV} = \frac{n_{s,r}(m_1) n_{s,r}(m_2) \Delta t g(\log P)}{1 + \delta_{1,2}} \times \int_0^{v_{e,r}} (1 - F_{\text{coll},v}) v \sigma_{\text{tc}} f(v, r) d^3 v,$$

where $\delta_{1,2}$ is the Kronecker delta which is unity if stellar type 1 and 2 are identical and zero otherwise. The quantity $F_{\text{coll},v}$ is the fraction of collisions which lead to the formation of an unstable binary system whose natural evolution is the coalescence in a single massive star (see Section 2.6) and can be written as

$$F_{\text{coll},v} = \frac{\sigma_{\text{coll}}}{\sigma_{\text{tc}}}.$$

As can be seen from the above equations, the binary systems formed via tidal capture are assumed to follow the original period distribution.

2.3 Collisional hardening and binaries ionization

When a single star collides with a binary systems, the two objects exchange part of their energy. In particular, the colliding star

¹ I did not assumed a criterion to link the upper truncation of the period distribution to the local velocity dispersion, assuming that binaries born in all clusters with the same initial properties.

gain (lose) a fraction of its kinetic energy, which is balanced by an decrease (increase) of the binary system binding energy, if the *hardness parameter*

$$\eta = \frac{E_b}{m_s \sigma_{v,r}^2}, \quad \text{where} \quad E_b = \frac{G m_1 m_2}{2 a} \quad (3)$$

is larger (smaller) than unity (Heggie 1975). The variation of binding energy of the binary system translates into a change in the period (i.e. in the orbital separation). This process is called ‘collisional hardening (softening)’. If the binding energy of the binary system drops to zero then the binary is disrupted (binary ionization).

The code follows the evolution of the binding energy of each sub-population of binaries and calculates the number of binaries which undergo ionization. In particular, the fraction of binding energy gained (lost) by the binary system after a time interval Δt has been assumed to be

$$\frac{\Delta E_b}{E_b} \sim \Delta t \int_0^{r_{\text{rel}}} n_{b,r}(m_1, m_2, \log P) \left(\frac{1}{E_b} \frac{dE_b}{dt} \right)_r d^3 r$$

and

$$\left(\frac{1}{E_b} \frac{dE_b}{dt} \right)_r = \begin{cases} \frac{7.6\sqrt{\pi} G a (n_s m_s)}{\sigma_{v,r}} & \text{if } \eta > 1 \\ -\frac{16\sqrt{\pi} G a (n_s m_s^2) \log \Lambda}{\sigma_{v,r}(m_1 + m_2)} & \text{if } \eta < 1 \end{cases}$$

(Binney & Tremaine 1987; Hills 1992).

Here the quantities $\langle X \rangle$ indicates the mean value of X measured at the radius r . I assumed $\Lambda = 1/\eta$, which is a suitable choice for $\eta < 1$ (Binney & Tremaine 1987). I neglected the change of the binary eccentricity distribution due to collisions.

Collisions between binaries play also an important role, in particular when high primordial binary fractions are considered. Binary–binary interactions are very efficient for ionizing one (or both) of the two binaries (Mikkola 1983a; Sweatman 2007). In a collision between binaries the most probable outcome is the disruption of the softer binary and hardening of the harder one. As a first-order approximation, the collisions between two binary systems have been treated as normal collisions between a binary and a single point-mass object with a mass equal to the systemic mass of the colliding binary system ($m_1 + m_2$). Note that this simplification underestimates the amount of energy transferred between the two binaries since the geometrical part of the cross-sections defined above would be few times larger than what assumed. Moreover, under this assumption only one of the various possible outcomes of a binary–binary collision is considered (see Fregeau et al. 2004). However, despite the adopted simplifications, the treatment described above accounts for most of the contribution of collisions between binaries to the ionization process.

Similarly, the variation of periods and semi-axes have been calculated considering that

$$\frac{\Delta a}{a} = -\frac{\Delta E_b}{E_b} \quad \text{and} \quad \Delta \log P = -\frac{2 \ln 10}{3} \frac{\Delta E_b}{E_b}. \quad (4)$$

2.4 Exchanges

A possible occurrence in a collision between a single star and a binary system consists in the formation of an unstable triple system which naturally evolves by expelling one of the components (usually the least massive) of the original system. The number of exchanges has been estimated by means of the cross-section σ_{exch} provided by Heggie, Hut & McMillan (1996) (see their equations 4 and 17). Since this formulation is valid only in the case $\eta > 1$, I calculated

the number of exchanges only in this regime. On the other hand, the process of exchange in soft binaries is largely less efficient than the one of ionization and can be neglected. Therefore, the number of exchanges involving an hard binary having components of masses m_1 and m_2 and period P with a colliding star with mass m_s is

$$\Delta N_{\text{exch}}(m_1, m_2, m_s, \log P) = \int_0^{r_{\text{rel}}} \frac{dN_{\text{exch}}}{dr} d^3 r$$

with

$$\frac{dN_{\text{exch}}}{dr} = n_{s,r}(m_s) n_{b,r}(m_1, m_2, \log P) \Delta t \times \int_0^{v_{e,r}} v \sigma_{\text{exch}} f(v, r) d^3 v$$

At each time-step, the number of binary systems and single stars have been corrected for this effect.

2.5 Stellar evolution

As time passes, most stars evolve and die after time-scales which depend mainly on the star’s mass. Massive stars ($M > 7 M_{\odot}$) at the end of their evolution explodes as SNII. Less massive stars suffer strong mass-losses during their latest stages of evolution and terminate their evolution as white dwarf (WD).

When a star belonging to a binary system evolves there are many possible outcomes. If the mass of the primary star is large enough to produce a SNII explosion part of the elapsed energy is converted in a velocity kick that increase the total energy of the system. If the total energy (potential and kinetic) is positive then the system is disrupted and its components will evolve separately. Else, the system remains in a bound state in which one of the two companions is the compact remnant of the evolved star.

Otherwise, if the primary component of the binary system is small enough to avoid the ignition of the triple- α cycle, mass-losses produce a rapid halting of the nuclear reactions leading to the formation of a WD. Given the large number of low-mass stars, this event is the most probable among the various possible outcomes.

In particular, I considered two important cases: (i) the envelope of the evolving stars reach the Roche-lobe of the companion, igniting the process of mass transfer (see Section 2.6); (ii) the star follows an unperturbed evolution leading to the formation of a binary system formed by a WD and a companion.

To account for these processes, at each time-step of the simulation, a limiting mass has been associated. Then, for each mass bin, the code calculates the fraction of stars with masses larger than this limiting mass, assuming the stars to populate uniformly the mass bin. When this process takes place in a binary system, the occurrence of the various possible processes described above has been considered. In particular, in the case of a massive primary component I followed the prescriptions of Belczynski, Kalogera & Bulik (2002). In the case of binary systems formed by low-mass stars a distinction between processes (i) and (ii) has been made using the criterion described in Section 2.6. The amount of mass lost at the end of the evolution has been calculated using the prescriptions by Weidemann (2000).

The number of binary and single stars is updated accordingly.

2.6 Direct collisions and coalescence

From the early 1950s it is well known that in globular clusters exists a population of massive objects that, in the colour–magnitude diagram, lie along an extension of the main sequence, in a region

which is brighter and bluer than the turn-off (Piotto et al. 2004, and references therein). These stars are called Blue Straggler Stars (BSSs). Two mechanisms have been proposed to explain the origin of these stars: (I) direct collision between two single stars (Hills & Day 1976) and (II) mass transfer activity in close binary systems (McCrea 1964).

Case (I) occurs if the impact parameter of the collision between two single stars is small enough to form an unstable system in which the process of mass transfer leads to the formation of a single massive star.

In case (II) when the orbital separation of a binary system reduces to a critical distance, the binary system became unstable and the ignition of the process of stable mass transfer occurs. This phenomenon can be induced by two different mechanisms: (IIa) collisional hardening (see Section 2.3) and (IIb) off-main-sequence evolution of the primary component of the binary system. In the former case, hard binaries subject to a high number of collisions tend to reduce their orbital separation (see equation 4). In the latter case, when the primary component of the binary system exhausts the hydrogen in its core, it expands its envelope by a large factor (which depends on its mass) possibly reaching the Roche radius of the secondary component.

The critical distance between two companions in a binary system to ignite stable mass transfer is

$$a_{\min} = 2.17 \left(\frac{m_1 + m_2}{m_2} \right)^{1/3} R_2 \quad (\text{Lee Nelson 1988}).$$

The final product of these processes is a system containing a massive star having a mass $m_1 < m < (m_1 + m_2)$. The formation of BSSs affects the number of binary and single stars.

To evaluate the frequency of the processes described above, I first consider the cross-section σ_{coll} for a stellar collision which leads to a close binary system with orbital separation $a < a_{\min}$ (case I). This cross-section has been calculated using the formulation by Lee & Ostriker (1986; see their equations 2.8 and 4.12):

$$\sigma_{\text{coll}} = \pi a_{\min} \frac{2Gm_2}{v^2}.$$

Then, the number of coalesced stars via direct collision can be written as

$$\Delta N_b(m_1, m_2, \log P) = \int_0^{r_{\text{rel}}} \frac{dN_{b,\text{coll}}(m_1, m_2)}{dr} d^3r,$$

where

$$\frac{dN_{b,\text{coll}}}{dr} = \frac{n_{s,r}(m_1) n_{s,r}(m_2) \Delta t}{1 + \delta_{1,2}} \int_0^{v_{e,r}} v \sigma_{\text{coll}} f(v, r) d^3v.$$

The fraction of coalesced stars via collisional hardening (case IIa) has been calculated by following the evolution of the semi-axes of the binary population (see Section 2.3). Instead, when the coalescence is due to the evolution of the primary star of a binary system (case IIb), the code calculates the fraction of system with an evolving primary star which satisfies the condition

$$a < a_{\min} \frac{R_{1,\text{max}}}{R_1},$$

where R_1 and $R_{1,\text{max}}$ are the radii of the primary star during its quiescent and evolved stages, respectively.

2.7 Evaporation

During its evolution, a globular cluster undertakes the tidal stress of its host galaxy. As a result of this interaction, it loses part of its stellar systems decreasing its total mass. The rate of evaporating

systems depends on the cluster orbit and on its structural parameters (Gnedin & Ostriker 1997).

Here, the treatment of evaporation has been greatly simplified assuming the cluster to lose a constant fraction ν of its objects during all its evolution. Although this is a crude approximation, it can be used to simulate the effect of a tidal field on the relative amount of single and binary stars survived to the evaporation process. A homogeneous evaporation rate is also in agreement with the most recent N -body simulation (Hurley et al. 2007; Kim et al. 2008). At a given distance from the cluster centre, I assumed the velocity distribution of a population of objects with mass m can be well represented by a Maxwellian distribution²

$$f(v, r) = A e^{-v^2/2K},$$

where K is a term proportional to σ^2 and A is a normalization factor. The quantity K depends on the stellar mass according to the status of relaxation of the cluster (see Appendix A).

The relative number of evaporating systems belonging to a given group of mass can be therefore calculated by integrating over the entire cluster extension the fraction of stars with a velocity higher than the escape velocity ($v_{e,r} = \sqrt{-2\Phi_r}$):

$$N'(m) = B \int_0^{r_t} n_r(m) \frac{dv'(m)}{dr} d^3r,$$

where

$$\frac{dv'(m)}{dr} = \int_{\beta W_r(m)}^{+\infty} y^{1/2} e^{-y} dy,$$

$$W_r(m) = -\frac{\Phi_r}{\sigma_{v,0}^2}.$$

The term β accounts for the state of partial relaxation (see Appendix A)

$$\beta = \frac{m}{[\gamma \langle m \rangle + (1 - \gamma)m]},$$

where

$$\gamma = \frac{N_m(r < r_{\text{rel}})}{N_m}$$

is the fraction of stars with mass m located in the region where relaxation already occurred.

Once this ratios are calculated for all the mass groups, the normalization factor B can be derived by imposing that

$$\Delta N_{\text{sys}} = \sum_i N'(m_i) = \nu N_{\text{sys}}.$$

2.8 Cluster dynamical evolution

During its evolution, the cluster core loses part of its mass as a result of the processes of mass segregation and evaporation. To maintain its virial equilibrium the cluster collapses increasing its central density and velocity dispersion. A significant population of hard binaries feeds kinetic energy into the cluster through binary–single and binary–binary interactions which counteract the effects of evaporation. This process can halt and even reverse the contraction of the core (Hills 1975; Gao et al. 1991). Fregeau et al. (2003) showed that also a small fraction of hard binaries is sufficient to support the core against collapse significantly beyond the normal core-collapse time.

² Although this assumption holds only in the core, I extended its validity to the entire cluster only to calculate the relative fraction of evaporating stars belonging to different mass groups.

I considered the evolution of the structural properties of the cluster in a highly simplified way. In particular, the code calculates at each time-step of the simulation the number of stars contained in the cluster core and updates the core radius and the central velocity dispersion using the relations

$$\frac{r'_c}{r_c} = \frac{E}{E'} \left(\frac{N'}{N} \right)^2 \quad \text{and}$$

$$\frac{\sigma'_{v,0}}{\sigma_{v,0}} = \left(\frac{E' N}{E N'} \right)^{1/2},$$

where

$$\frac{E'}{E} = \left[\frac{\ln(N'/2)}{\ln(N/2)} \right]^{88 z(\xi)}$$

(Hills 1975).

Here the symbols X and X' indicate the values of X in two subsequent time-steps. The term E'/E represents the ratio between the cluster binding energies in two subsequent time-steps due to the contribution of binaries. Here, all quantities refers to the cluster core and ξ refers to the fraction of hard binaries. The exponent $z(\xi)$ is related to the heating of binaries due to binary–single stars and binary–binary interaction and can be written as

$$z(\xi) = (\xi/1.3) + 10.3 \xi^2 (1.2 - 1/\langle \eta \rangle) \quad (\text{Mikkola 1983b}).$$

Moreover, the King parameter has been updated using equation (2). In this way, the cluster structural parameters satisfy the virial theorem during all the simulation.

In Fig. 1 the evolution of the core radius for the models s5p3e5f50 and s5p3e5f10 are shown. As can be seen, the general trend of the core radius evolution is characterized by a progressive contraction of the core induced by the ever continuing losses of stars. In model s5p3e5f50 the heat generated by hard binaries halts the contraction and leads to a stabilization toward an equilibrium value. The behaviour of the evolution of the cluster characteristic radii qualitatively agree quite well with the most recent N -body simulation computations (see Fregeau et al. 2003; Kim et al. 2008). The details

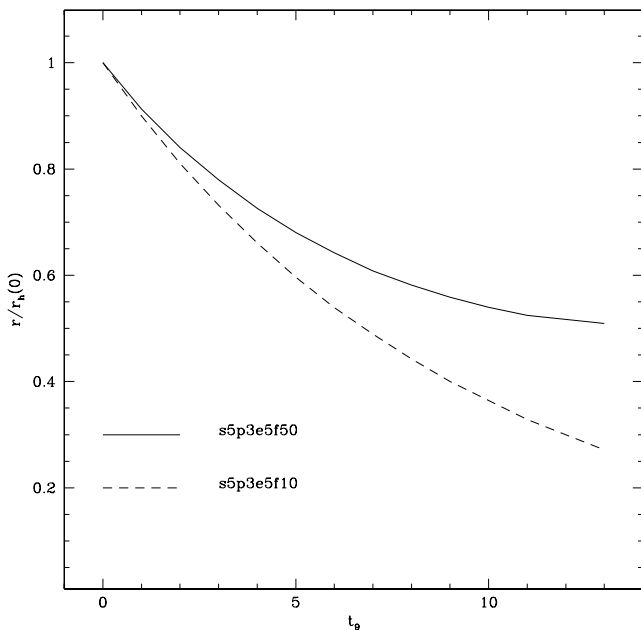


Figure 1. The evolution of the core radius is shown as a function of time for the models s5p3e5f50 (solid line) and s5p3e5f10 (dashed line).

of the core oscillations and post-collapse evolution are not reproduced by the code as a consequence of the simplified treatment described above. However, this should have only a minor effect on the predicted evolution of the properties of the binary population.

3 RESULTS AND DEPENDENCE ON THE ASSUMPTIONS

I run a set of 36 simulations spanning a wide range in density, velocity dispersion, evaporation efficiency and initial binary fraction. A list of all the performed simulations and their initial and final parameters is provided in Table 1.

To test the dependence of the obtained results on the adopted assumptions in the following subsections I compare the model s5p3e5f50 with a set of simulations performed with the same initial conditions but different assumptions. The results of these additional simulations are listed in Table 2.

3.1 Dependence on metallicity

As described in Section 2.1, the simulations have been performed adopting a metal mass fraction $Z = 10^{-3}$. Metallicity influences both the evolutionary time-scales and the mass–radius relation and can in principle affect the evolution of the binary population.

In the upper panels of Fig. 2 the behaviour of the binary fraction as a function of time is showed for the model s5p3e5f50 and for a simulation performed with $Z = 10^{-4}$. As can be noted, the two models are indistinguishable even when the core binary fraction is considered. Also the final binary fraction of the metal-poor model is the consistent with the reference metal-rich one within 0.3 per cent (see Table 2).

I conclude that the metallicity plays a negligible role in the evolution of the binary fraction in the presented simulations. Note however that metallicity can play an important role in the primordial fraction of binaries and in the formation of X-ray binaries (see Ivanova 2006). In the models presented here such effects can remain hidden because of the adopted simplifications.

3.2 Dependence on the IMF

Another important ingredient of the simulations is the IMF. Indeed, it determines the relative fraction of each mass group and influences the distribution of mass ratios.

Although the power-law exponent of the IMF is well established for stars with masses $M > 0.5 M_{\odot}$, there are still large uncertainties in the shape of the low-mass end of the IMF. Moreover, some authors claim a dependence of the power-law exponent of the low-mass end of the IMF on metallicity (McClure et al. 1986; Djorgovski, Piotto & Capaccioli 1993).

In the central panels of Fig. 2 the model s5p3e5f50 is compared with two simulations performed using two extreme values of the IMF power-law exponent in the mass range $M < 0.5 M_{\odot}$ ($\alpha = 0$ and 1.8). As can be seen, the three models show a very similar behaviour during all the cluster evolution. The final binary fractions of the three models are also compatible within ~ 5 per cent.

Therefore, although the IMF plays a fundamental role in the determinations of the main characteristics of the binary population, it plays only a minor role in the evolution of the binary fraction.

Table 1. Complete list of simulations.

Model ID	Initial conditions			Final conditions		
	$\log \rho_0$ ($M_{\odot} \text{ pc}^{-3}$)	$\sigma_{v,0}$ (km s^{-1})	ξ (per cent)	ν (per cent Gyr^{-1})	ξ (per cent)	ξ_c (per cent)
s2p1e0f10	1	2	10	0	8.3	12.4
s3p2e0f10	2	3	10	0	6.6	10.7
s5p2e0f10	2	5	10	0	6.6	10.0
s5p3e0f10	3	5	10	0	4.7	7.8
s5p4e0f10	4	5	10	0	2.8	5.3
s5p5e0f10	5	5	10	0	2.1	4.3
s9p4e0f10	4	9	10	0	2.9	5.0
s9p5e0f10	5	9	10	0	1.7	3.3
s13p5e0f10	5	13	10	0	1.6	2.9
s2p1e5f10	1	2	10	5	10.3	14.7
s3p2e5f10	2	3	10	5	7.5	11.0
s5p2e5f10	2	5	10	5	6.8	9.9
s5p3e5f10	3	5	10	5	4.8	7.6
s5p4e5f10	4	5	10	5	4.1	6.9
s5p5e5f10	5	5	10	5	3.1	5.7
s9p4e5f10	4	9	10	5	3.0	4.9
s9p5e5f10	5	9	10	5	2.5	4.1
s13p5e5f10	5	13	10	5	2.3	3.8
s2p1e0f50	1	2	50	0	40.9	51.5
s3p2e0f50	2	3	50	0	30.6	42.5
s5p2e0f50	2	5	50	0	31.5	41.8
s5p3e0f50	3	5	50	0	20.0	30.2
s5p4e0f50	4	5	50	0	12.1	21.0
s5p5e0f50	5	5	50	0	9.3	17.4
s9p4e0f50	4	9	50	0	11.6	18.8
s9p5e0f50	5	9	50	0	6.6	12.3
s13p5e0f50	5	13	50	0	6.0	10.5
s2p1e5f50	1	2	50	5	56.0	64.3
s3p2e5f50	2	3	50	5	44.6	53.8
s5p2e5f50	2	5	50	5	28.0	37.2
s5p3e5f50	3	5	50	5	29.9	39.0
s5p4e5f50	4	5	50	5	16.6	25.0
s5p5e5f50	5	5	50	5	11.5	20.2
s9p4e5f50	4	9	50	5	14.3	22.0
s9p5e5f50	5	9	50	5	8.2	13.5
s13p5e5f50	5	13	50	5	7.9	12.7

Table 2. Results of the test simulations.

Model ID	Initial conditions				Final conditions		
	ξ (per cent)	$\log Z$	α ($M < 0.5 M_{\odot}$)	$g(\log P)$	$\log P_{\text{max}}$ (d)	ξ (per cent)	ξ_c (per cent)
s5p3e5f50	50	-3	1.3	Gaussian	7	29.9	39.0
s5p3e5f50.zlow	50	-4	1.3	Gaussian	7	30.0	39.3
s5p3e5f50.m18	50	-3	1.8	Gaussian	7	24.9	35.7
s5p3e5f50.m0	50	-3	0.0	Gaussian	7	31.3	41.2
s5p3e5f50.pflat	50	-3	1.3	Flat	7	39.8	48.3
s5p3e5f50.p6	50	-3	1.3	Gaussian	6	35.2	44.9

3.3 Dependence on the period distribution

One of the most important assumptions made in the simulations regards the distribution of periods of the binary population. The shape and the extremes of this distribution determine the ratio of soft-to-hard binaries (i.e. the fraction of binaries which can undergo ionization).

To evaluate the impact of these assumptions on the evolution of the binary fraction I compared the model s5p3e5f50 with two sim-

ulations performed assuming (i) a flat period distribution truncated at $\log P(d) = 7$ (where P is expressed in days) and (ii) a lognormal distribution truncated at $\log P(d) = 6$. The results of this comparison are shown in the lower panels of Fig. 2. Note that, while a variation of the upper limit of the period distribution produces only small changes ($\Delta\xi < 6$ per cent) in the final binary fraction, the model with a flat period distribution maintains a significantly higher fraction of binary systems during all the cluster evolution. In particular, after 13 Gyr, this last model contains ~ 10 per cent of binaries more

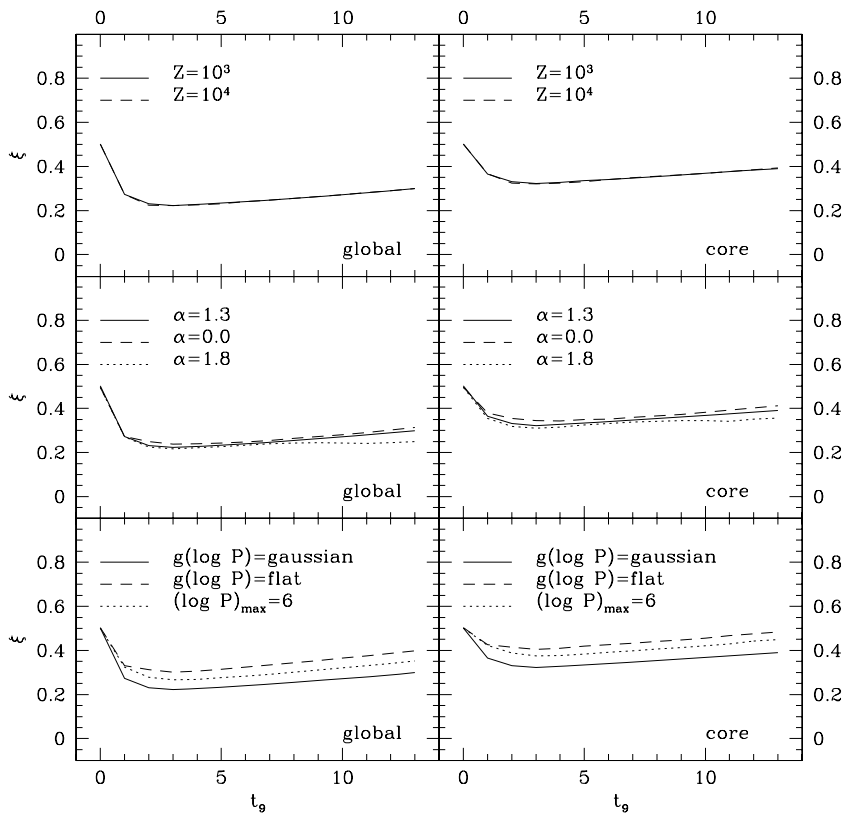


Figure 2. The evolution of the binary fraction is shown as a function of time for the reference model s5p3e5f50 (solid lines) and for the models calculated under different assumptions. Left-hand panels show the binary evolution in the whole cluster, right-hand panels show the binary evolution in the cluster core.

than the reference model. As pointed out above, this effect is due to the higher fraction of hard binaries resulting from the flat distribution of periods (60 per cent at the beginning of the simulation) with respect to the lognormal distribution (43 per cent).

All the results presented in the following sections are based on simulations run assuming a lognormal distribution of periods truncated at $\log P(d) = 7$. Although the dependence of the properties of the binary population on the cluster structural and environmental parameters should not be influenced by this choice, it is important to bear in mind that the absolute results of the individual simulations are highly sensitive to this assumption.

4 EVOLUTION OF THE BINARY FRACTION

The simulations listed in Table 1 cover a range of structural and environmental parameters comparable to those spanned by Galactic globular clusters. Thus, they can be used to study the efficiencies of the various processes of binary formation/destruction as a function of the initial conditions.

For this purpose consider the derivative

$$\frac{d\xi}{dt_g} = \sum_X \left(\frac{d\xi}{dt_g} \right)_X.$$

This quantity can be seen as the sum of the contributions of the individual processes, where

$$\left(\frac{d\xi}{dt_g} \right)_X = \frac{N_{\text{sys}} d_X N_b - N_b d_X N_{\text{sys}}}{N_{\text{sys}}^2}$$

represents the contribution of the process X to the above derivative. In Fig. 3 the behaviour of the derivatives defined above are shown

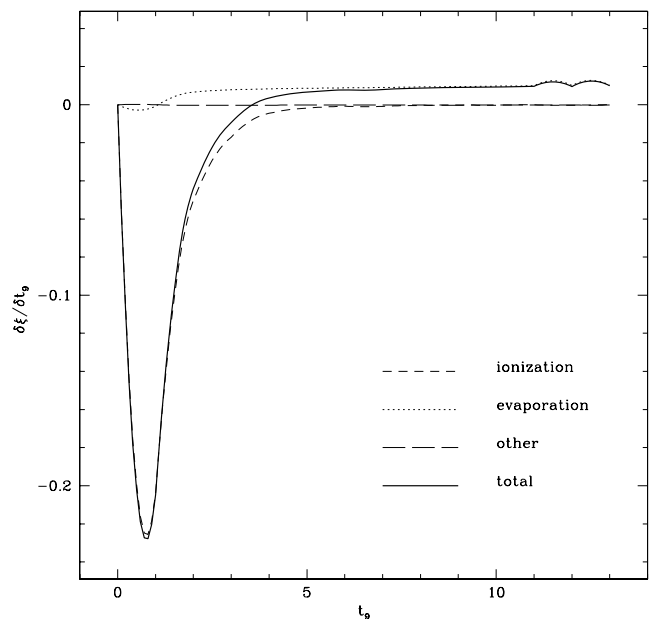


Figure 3. Derivative of the binary fraction as a function of time for model s5p3e5f50. The contributions of the various processes are indicated.

as a function of time for the model s5p3e5f50. Such a behaviour is qualitatively the same in the other models with different initial conditions. As can be noted, the process of ionization is the main responsible for the variation of the binary fraction reaching its maximum efficiency in the first Gyr of evolution. Another important

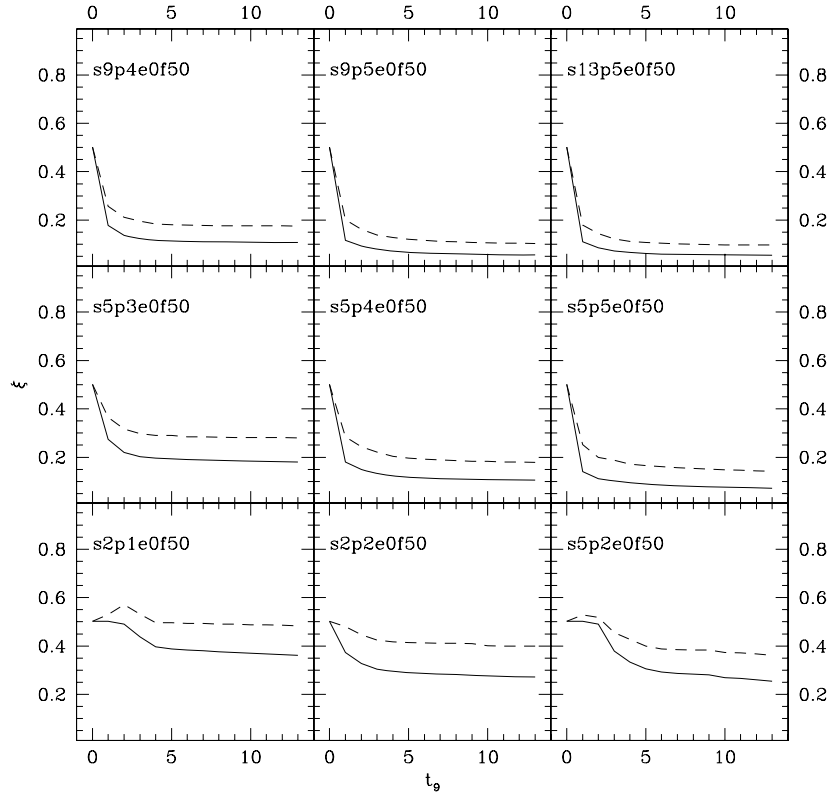


Figure 4. The evolution of the binary fraction in the core (dashed lines) and in the whole cluster (solid lines) are shown as a function of time for all the models with $\nu = 0$ and $\xi = 50$ per cent.

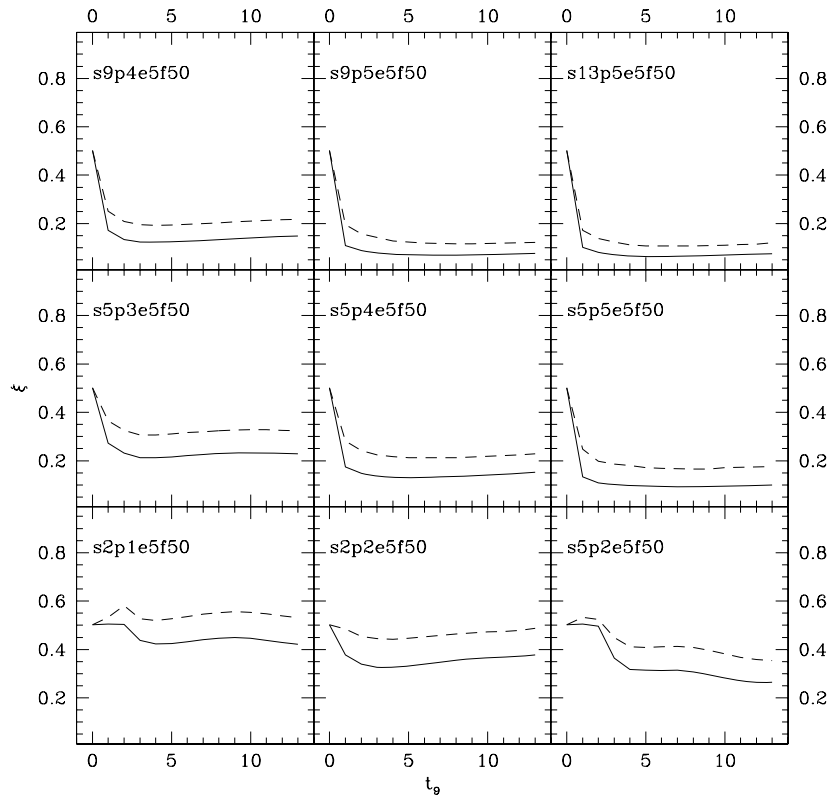


Figure 5. Same of Fig. 4 but for all the models with $\nu = 5$ per cent Gyr^{-1} and $\xi = 50$ per cent.

contribution is given by evaporation (in models where $\nu \neq 0$) which enhances the fraction of binaries systematically during the whole cluster evolution. All the other processes play only a minor role.

In Figs 4 and 5 the behaviour of the binary fraction as a function of time is shown for all the simulations with initial binary fraction $\xi = 50$ per cent. As can be noted, the general evolution of the binary fraction is characterized by a sudden decrease in the first Gyr, followed by a constant trend during the subsequent Gyr of evolution. In simulations run assuming $\nu \neq 0$, the fraction of binaries slightly increase in the last Gyr of evolution. The fraction of binaries in the core is systematically larger than that of the entire cluster. This difference is more evident after 2–3 Gyr evolution.

The strong initial decrease of the binary fraction is due to the process of binary ionization which destroys a large fraction of binaries during the first Gyr of evolution. After this initial stage, all the soft binaries have been destroyed and the evolution of the binary fraction is driven by the other processes which have a smaller efficiency. In particular, if the efficiency of the process of evaporation is large, the fraction of binaries increases again. Binary systems are in fact on average more massive than single stars and tend to have therefore smaller velocities. Therefore, a larger number of single stars reach the cluster escape velocity with respect to binary systems, thus increasing the relative fraction of binaries. As relaxation

proceeds a larger fraction of binaries sink into the central regions of the cluster, as a consequence of the process of mass segregation, thus increasing the core binary fraction.

Fig. 6 shows a map of the fraction of surviving binary systems after 13 Gyr in the $\log \rho_0 - \sigma_{v,0}$ plane for the simulations with initial binary fraction $\xi = 50$ per cent. As can be seen, a clear trend is visible as a function of the cluster final conditions. In particular,

- (i) the fraction of binaries decreases by increasing the central velocity dispersion;
- (ii) the fraction of binaries decreases by increasing the central density;
- (iii) the fraction of binaries increases by increasing the efficiency of the evaporation.

The physical reasons at the basis of these trends are linked to the efficiencies of the processes of binary ionization and evaporation. Indeed, by increasing the cluster velocity dispersion increase the ratio of soft-to-hard binaries (see equation 3) which are destroyed by the process of ionization in the first Gyr of evolution. The efficiency of ionization increase also by increasing the cluster density (see Section 2.3). On the other hand, evaporation tends to increase the fraction of binaries (see above).

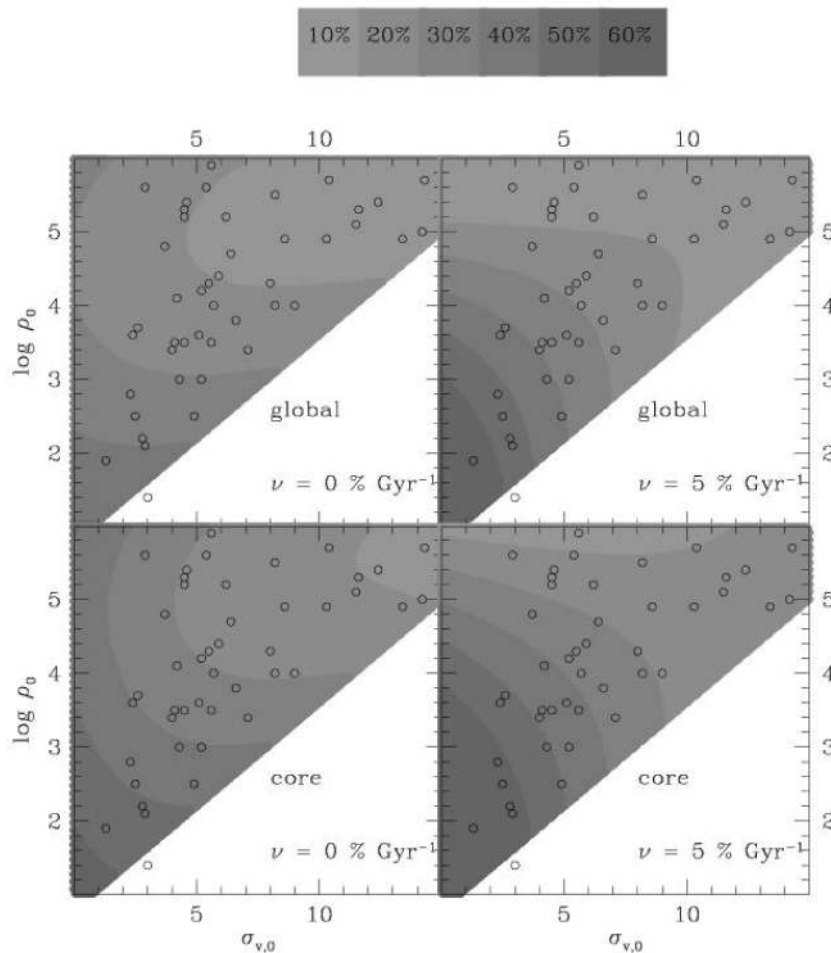


Figure 6. Maps of the surviving binary fraction in the plane $\log \rho_0 - \sigma_{v,0}$ for $\xi = 50$ per cent, $\nu = 0$ (left-hand panels) and $\nu = 5$ per cent Gyr^{-1} (right-hand panels). Lower panels refer to the core binary fraction, upper panels to the whole cluster binary fraction. Darker regions indicate higher binary fractions in steps of 10 per cent. The locations of the Galactic globular clusters (from Djorgovski 1993) are also marked with open circles.

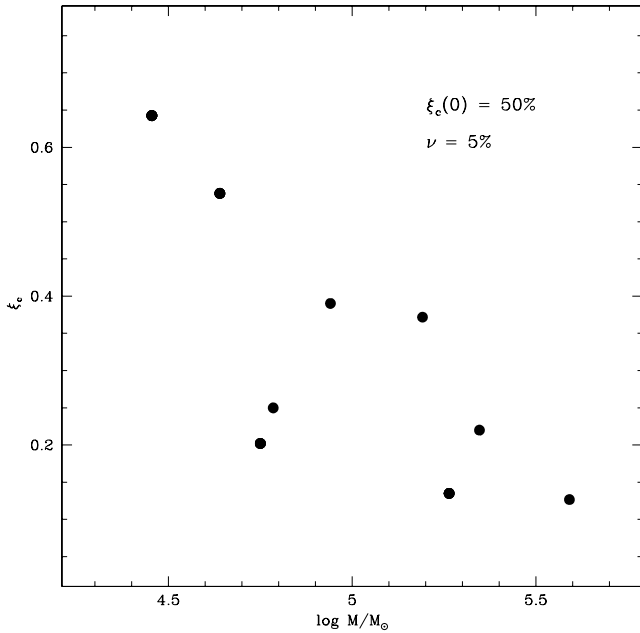


Figure 7. The surviving fraction of binaries after 13 Gyr is shown as a function of the residual cluster mass for all the models with $\xi = 50$ per cent and $\nu = 5$ per cent. A clear anticorrelation between these quantities is visible.

Interestingly, the efficiency of ionization and the cluster mass have the same dependences on the cluster structural parameters (ρ_0 and $\sigma_{v,0}$). Indeed, more massive clusters have, on average, larger densities and velocity dispersions (Djorgovski & Meylan 1993). In Fig. 7 the fraction of binaries after 13 Gyr is plotted against the residual cluster mass for all models with $\xi = 50$ per cent and $\nu = 5$ per cent. As expected, a clear anticorrelation is clearly visible between these two quantities. The same result can be achieved considering different values of the primordial binary fraction and evaporation efficiency.

In Fig. 8 the evolution of the binary fraction for the model s5p3e5f50 is compared with that calculated for a model with the same initial conditions but a significantly smaller initial binary fraction (model s5p3e5f10). The binary fractions for the two models have been normalized to their initial values in order to compare the relative trend of their evolution. Note that the model which starts with a lower binary fraction maintaining a larger fraction of binaries in the first stages of its evolution. This evidence is more evident when the core binary fraction is considered. This is a consequence of two effects: (i) the effect of the binary–binary collisions and (ii) the dependence of the local relaxation time on the mean stellar mass (see equation 1). Indeed, in clusters with higher binary fractions, binary–binary collisions are ~ 25 times more frequent and, given their higher energetic budget, dominate the process of binary ionization. Moreover, the mean stellar mass is smaller in clusters with smaller binary fractions. The local relaxation time in these clusters is therefore longer, and a smaller fraction of binaries is therefore involved in the process of binaries destruction. This effect is amplified in the core where more binaries sink as a result of mass segregation. The trend is reversed after few Gyr when the impact of evaporation became more important. In fact, models with higher fractions of binaries tend to maintain binaries more efficiently. At the end of the simulation the two models contain a similar fraction of their initial budget of binaries in the core regardless of their primordial

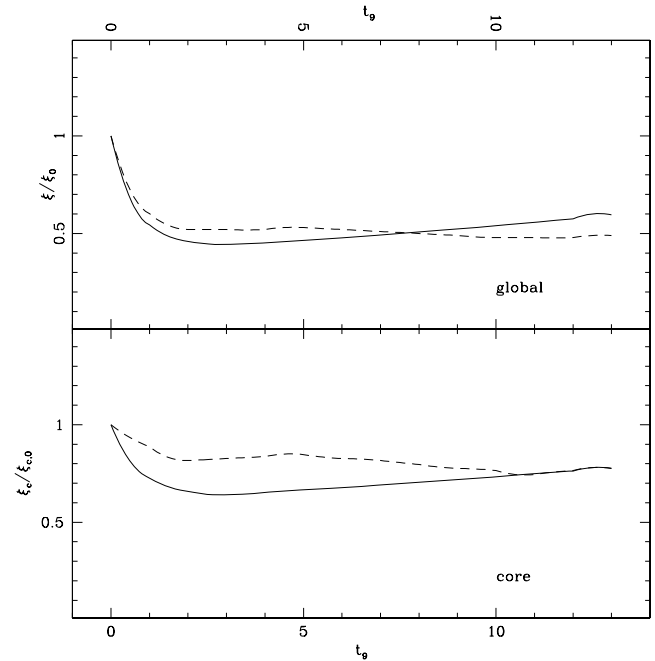


Figure 8. The binary fraction normalized to the initial value is shown as a function of time for the model s5p3e5f50 (solid lines) and s5p3e5f10 (dashed lines). The upper panel refers to the entire cluster, the lower panel to the cluster core.

content. In the following I discuss the dependence of the evolution of the binary population considering the models calculated assuming an initial binary fraction $\xi = 50$ per cent. The conclusions are qualitatively the same for the models with a smaller initial binary fraction.

5 RADIAL DISTRIBUTION OF BINARIES

Binary systems are on average more massive than single stars. Therefore, they are expected to have a different radial distribution with respect to single stars, as a result of the process of mass segregation.

Fig. 9 shows the fraction of binaries (model s5p3e5f50) normalized to the central value as a function of the radial distance from the cluster centre at different times. As expected, the fraction of binaries shows a central peak, decreasing toward the external regions of the cluster. As time passes, relaxation occurs in the external regions and the cluster increases its concentration as a result of the ever continuing losses of stars. Consequently, the fraction of binaries populating the outermost part of the cluster slightly increases.

In Fig. 10 the radial behaviour of the normalized fraction of binaries (model s5p3e5f50) calculated after 13 Gyr is compared with models with extremely different initial conditions (models s2p1e5f50 and s13p5e5f50; upper panel) and with a smaller evaporation efficiency (s5p3e0f50; lower panel). Note that the slope of the decreasing trend of the binary fraction in the external part of the cluster is less steep in model s13p5e5f50 which undergo a stronger dynamical evolution. The same behaviour is visible when evaporation accelerates the cluster dynamical evolution.

Summarizing, the slope of the external decrease of the radial distribution of the binary fraction is steeper as the cluster is dynamically younger.

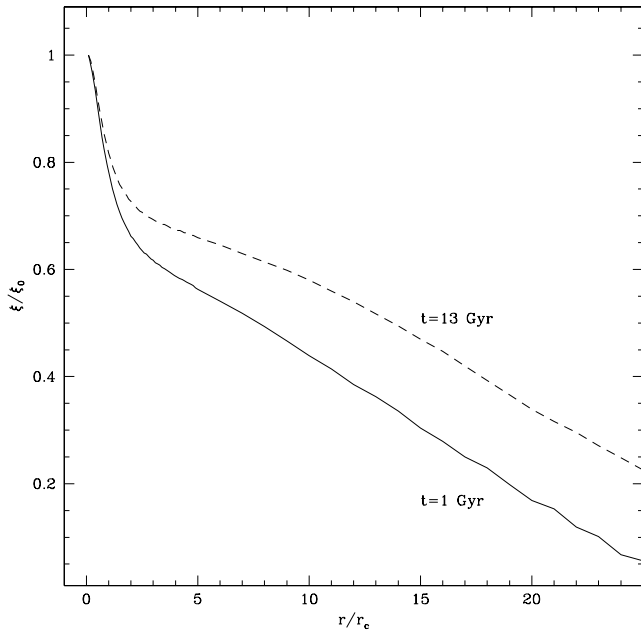


Figure 9. Normalized binary fraction as a function of the radial distance to the cluster centre at different times from the beginning of the simulation for the model s5p3e5f50.

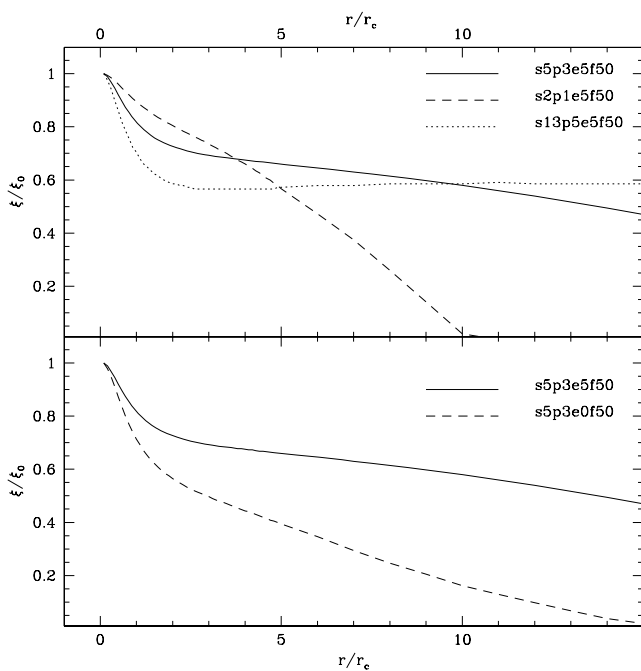


Figure 10. In the upper panel the comparison among the normalized binary fractions as a function of the radial distance to the cluster centre is shown for the model s5p3e5f50 (solid line), s2p1e5f50 (dashed line) and s13p5e5f50 (dotted line). The lower panel shows the same comparison but for the models s5p3e5f50 (solid line) and s5p3e0f50 (solid line).

A note of caution is worth taking: the code assumes that all the cluster stars follow the radial distribution predicted by a given King model according to their masses during the whole cluster evolution. Under this assumption, the process of mass segregation removes instantaneously all the radial differences in binary fraction produced

by the various mechanisms of binary formation/destruction. However, while this approximation is reasonable in the central regions (where the local relaxation time is relatively short) in the outer regions this assumption could not hold. Therefore, the predicted radial distribution of binaries could not be reliable in the external regions of the cluster.

6 PERIOD DISTRIBUTION

As outlined in Section 4, one of the main processes that drive the evolution of the binary fraction is the process of binary ionization. The binaries which are more subject to this process are those with smaller binding energy (i.e. longer periods). The shape of the distribution of periods therefore changes during the cluster evolution according to the efficiency of the process of binaries ionization.

In Fig. 11 the initial and final periods distributions of three models with different ionization efficiencies are shown. As expected, in models with a high ionization efficiency (see model s13p5e5f50) all binaries with $\log P(d) > 2$ are destroyed. On the opposite side, when ionization plays a minor role (model s2p1e5f50) a significant fraction of binaries with period as long as $\log P(d) = 6$ still survives.

7 MASS RATIO DISTRIBUTION

During the cluster evolution also the mass ratio distribution changes. There are three main processes that drive its evolution: stellar evolution, ionization and exchanges. Indeed, at the beginning of the simulation a large number of binaries are formed by a massive primary star which dies during the cluster evolution. The minimum possible mass ratio therefore increases with time. Moreover, the mean binding energy of the binary population is proportional to the average mass ratio. Thus, in clusters where ionization has a higher efficiency the mass ratio distribution should be more efficiently depleted up to larger values of q . During close encounters between a binary system and a massive colliding single star, the secondary star of the binary system is usually ejected from the system. When this process becomes frequent, the more stable systems against exchanges are those formed by equal-mass components. Thus, clusters with high collisional rates should show an increase of the number of equal-mass binaries.

In Fig. 12 the distribution mass ratios of the model s5p3f5e50 is compared with those of two models with extremely different densities (models s5p2e5f50 and s5p5e5f50) and evaporation efficiency (model s5p3e0f50). As expected, in all the distributions there are few systems with $q < 0.2$, as a result of stellar evolution. Moreover, the model s5p5e5f50 shows a lack of stars with low mass ratios with respect to the three other models. This is an effect of the high efficiency of ionization which depletes the distribution of mass ratios up to larger values of q . In none of the performed simulations an increase of the fraction of equal-mass binaries is noticeable. This means that the efficiency of the exchange process is rather low over the entire range of parameters spanned by the simulations. Indeed, even in the densest systems, where collisions are more frequent, the fraction of exchanges $N_{\text{exch}}/N_{\text{b}}$ never exceeds few per cent.

8 COMPARISON WITH *N*-BODY AND MONTE CARLO SIMULATIONS

The analytical model presented here has been compared with the most recent existing *N*-body (Hurley et al. 2007) and Monte Carlo (Ivanova et al. 2005) simulations. As outlined in Section 1, the

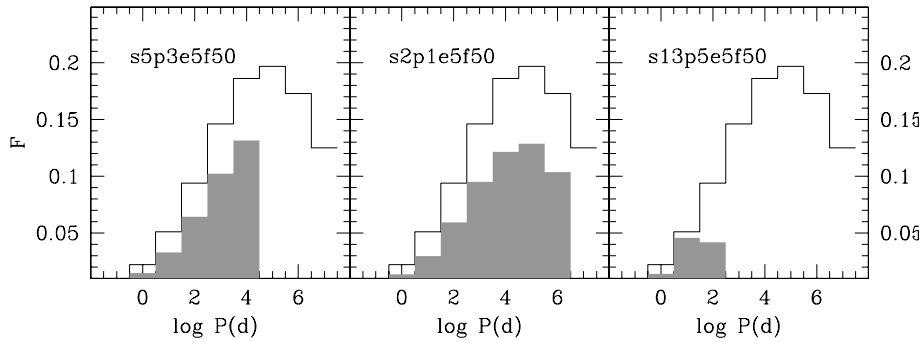


Figure 11. Period distributions of three different models. Grey histograms show the distribution after 13 Gyr. Open histograms show the distribution at the beginning of the simulation. Periods are expressed in days.

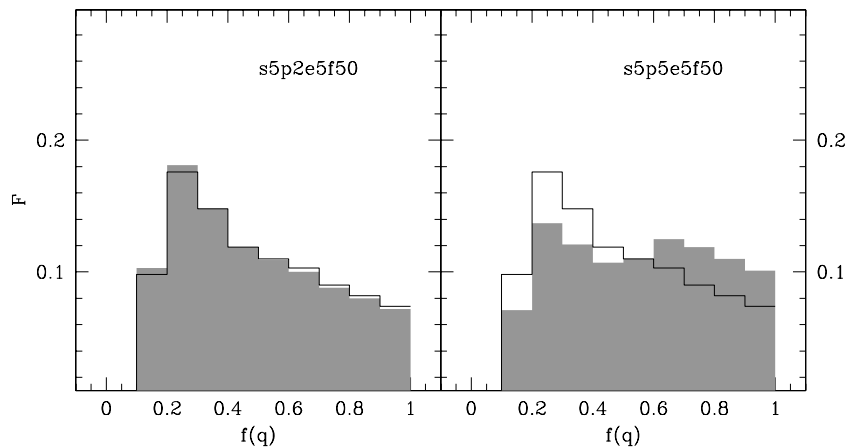


Figure 12. The mass ratio distributions after 13 Gyr of models s5p2e5f50 (left-hand panel) and s5p5e5f50 (right-hand panel) are shown with grey histograms. The mass ratio distribution of model s5p3e5f50 (open histograms) is shown in both *panels* for comparison.

two above approaches are completely different and lead to apparently discrepant results. In fact, while Monte Carlo simulations by Ivanova et al. (2005) predict a strong depletion of the core binary fraction, N -body simulations by Hurley et al. (2007) show the inverse trend.

Part of these discrepancies can be due to the very different initial conditions of the two simulations (Fregeau 2007). Indeed, Ivanova et al. (2005) simulated a series of high-density cluster with a significant velocity dispersion. In the following I refer to their model B05 which has $n = 10^5 \text{ pc}^{-3}$ and $\sigma_{v,0} = 10 \text{ km s}^{-1}$. In the approach followed by these authors, the evolution of the binary population is supposed to proceed in a ‘fixed background’ (i.e. a cluster whose structural parameters do not change during the simulation). The fraction of evaporating stars in these simulation is also very small (~ 6 per cent after 13 Gyr; N. Ivanova, private communication). This condition can be reproduced by assuming a very small efficiency of evaporation ($\nu \simeq 0$). Instead, Hurley et al. (2007) performed four different simulations assuming lower densities and velocity dispersions for cluster which interact with the Galactic disc on a circular orbit in the solar neighbourhood. I considered their model K24-50 which have an initial binary fraction $\xi = 50$ per cent a central star density $n = 100 \text{ pc}^{-3}$ and a velocity dispersion of $\sigma_{v,0} = 3 \text{ km s}^{-1}$. According to fig. 4 of Hurley et al. (2007), the cluster lose ~ 70 per cent of its object after 13 Gyr (comparable with a model with $\nu = 8$ per cent Gyr^{-1}). Considering the results obtained in Section 4 (see e.g. Fig. 6) the model of Hurley et al. is expected to retain much more binaries with respect to that of Ivanova et al. (2005).

Moreover, the two above authors make different assumptions regarding the distribution of periods. In fact, although both authors adopt a flat distribution, Ivanova et al. (2005) assume an upper truncation at $\log P(d) = 7$ while Hurley et al. (2007) impose an upper limit to the orbital distance of 50 au (corresponding to a truncation at $\log P(d) \sim 5$, see their fig. 2). Consequently, the model of Ivanova et al. contains a larger initial fraction of soft binaries which are easily destroyed during the cluster evolution.

To test the consistency of the approach followed in this paper with the ones quoted above, I run two simulations with the same assumptions and initial conditions of the above authors. I will refer to these two simulations as the H- and I-like models. Considering that both simulations start with an initial binary fraction $\xi = 50$ per cent, at the end of its evolution the H-like model contains a fraction of binaries in the core of $\xi = 76.9$ per cent while the I-like contains only a fraction of binaries $\xi = 25.1$ per cent. Although the absolute values of the above simulations differ from those reported by those authors, the qualitative behaviour of both simulations is well reproduced. This means that all the three approaches are qualitatively self-consistent, and that the observed discrepancy ($\Delta\xi \sim 52$ per cent) is due to both the intrinsic different starting parameters and the different assumptions.

To quantify the effect of the different assumptions on the resulting binary fraction, I performed a series of simulations adopting the starting conditions of the H-like and I-like models but different values of the maximum period and evaporation efficiency. The complete set of simulations are summarized in Table 3. As can be

Table 3. Results of the H- and I-like simulations.

Model ID	ξ (per cent)	$\log \rho_0$ ($M_\odot \text{ pc}^{-3}$)	Initial conditions			Final conditions	
			$\sigma_{v,0}$ (km s^{-1})	ν (per cent)	$\log P_{\text{max}}$ (d)	ξ (per cent)	ξ_c (per cent)
H-like	50	2.35	3	8	5	73.7	76.9
Hp7e8	50	2.35	3	8	7	56.3	61.7
Hp5e0	50	2.35	3	0	5	48.8	60.3
Hp7e0	50	2.35	3	0	7	33.8	45.8
I-like	50	5.4	10	0	7	15.7	25.1
Ip5e0	50	5.4	10	0	5	21.6	33.2

seen, adopting the same assumptions, the difference between the fractions of survived binaries predicted by the two models reduces by a factor of 2 ($\Delta\xi = 21\text{--}27$ per cent). Therefore, at least an half of the difference between the fractions of survived binaries predicted by the above models is due to the different assumptions. The remaining difference can be addressed to the different initial cluster conditions.

9 COMPARISON WITH OBSERVATIONS

The code described here has been used to interpret the observational evidence that young globular clusters contain a higher fraction of binaries with respect to older ones (Sollima et al. 2007). As outlined in Section 4, the fraction of binaries should not show significant variations in the last Gyr of evolution. Therefore, this trend could be due to (i) differences in the primordial binary fractions or (ii) to a different evolution of the binary populations linked to the different structural and environmental parameters of these two groups of clusters. Indeed, the group of young globular clusters of the sample of Sollima et al. (2007) is characterized by an age of $t_9 \sim 7$ Gyr, a mean central density $\langle \log \rho_0 \rangle = 0.65$ (where ρ_0 is expressed in $M_\odot \text{ pc}^{-3}$) and a velocity dispersion $\langle \sigma_{v,0} \rangle = 1.3 \text{ km s}^{-1}$ which are significantly different from those of the old group of that sample ($\langle t_9 \rangle = 11$, Gyr, $\langle \log \rho_0 \rangle = 2.15$ and $\langle \sigma_{v,0} \rangle = 3.3 \text{ km s}^{-1}$). According to the results found in Section 4, the group of young clusters should maintain a larger fraction of binaries during their evolution.

To test if these differences can be responsible for the difference in the observed binary fractions, I tried to reproduce the mean observed conditions of the two above groups of globular clusters assuming the same initial binary fraction. It is worth noting that the fraction of binaries derived by Sollima et al. (2007) is calculated in a restricted range of masses and mass ratios. To compare the results of the simulations with the observations, I compared the *minimum binary fraction* ξ_{min} defined in Sollima et al. (2007) with the ratio between the number of binaries with a primary star in the mass range $0.5 < m_1/M_\odot < 0.8$ and a mass ratio $q > 0.5$, and the number of objects in the same mass range. Of course, the relation between this quantity and the global binary fraction depends on the distribution of mass ratios. Given the arbitrary choice of this distribution (see Section 2.1) the absolute value of the initial fraction of binaries derived here is not reliable and can be only used for differential comparisons. According to Sollima et al. (2007), the groups of old and young globular clusters have *minimum binary fractions* $\xi_{\text{min}} = 6$ and 20 per cent, respectively.

The model that better reproduces the fraction of binaries in the old group of globular clusters after 11 Gyr is characterized by an initial binary fraction of $\xi = 8$ per cent. I found no combinations of the initial parameters able to reproduce the observed fraction of

binaries in the young group of globular clusters without assuming a larger initial binary fraction. This indicates that, although the dynamical status of the young group of globular clusters favours the survival of a larger fraction of binaries, the most of the observed difference have to be due to primordial differences in the cluster binary content.

10 CONCLUSIONS

I presented a code designed to simulate the evolution of the properties of a binary population in a dynamically evolving star cluster. A number of simulations spanning a wide range of structural and environmental parameters have been run.

In general, the fraction of binaries appears to decrease with time by a factor of 1–5, depending on the initial cluster parameters. In particular, the fraction of binaries quickly decreases in the first Gyr of evolution, as a result of the high efficiency of the ionization process in this initial stage.

The analysis of the contributions of each mechanism of formation and destruction of binaries indicates that the main processes that drive the evolution of the binary fraction in globular clusters are the processes of binary ionization and evaporation. This result seems to be confirmed by the observational fact that open clusters and low-density globular clusters contain more binary systems than dense high-velocity dispersion globular clusters (Sollima et al. 2007). As a consequence, the fraction of survived binaries increases when the cluster structural parameters support a lower efficiency of the process of ionization and in clusters subject to strong evaporation. Moreover, also the final distributions of periods and mass ratios change as a function of the cluster structural parameters. In particular, clusters with a higher efficiency of binary ionization tend to have binaries with shorter periods and higher mass ratios. At present, the range in central density and velocity dispersion spanned by the sample of globular clusters with homogeneous estimates of binary fraction is very small and does not allow a proper comparison (see Sollima et al. 2007). However, preliminary results by Milone et al. (2008) based on the analysis of a larger sample of globular clusters seems to confirm this trend. These authors found a significant anticorrelation between the fraction of binaries and the cluster luminosity (i.e. mass). Indeed, more massive clusters have, on average, larger densities and velocity dispersions (Djorgovski & Meylan 1993). Therefore, the observed anticorrelation could be due by the fact that the cluster mass and the efficiency of binary ionization have the same dependence on the cluster structural parameters (ρ_0 and $\sigma_{v,0}$).

The dependence of the obtained results on the assumptions has been tested. The evolution of the binary fraction appears to be non-sensitive to the assumed cluster metallicity and to the shape of the

low-mass end of the IMF. A significant dependence on the initial shape of the distribution of periods has been found. In particular, a difference of ~ 10 per cent has been found by switching from a lognormal to a flat distribution. Therefore, the decreasing trend of the binary fraction with time could be even inverted assuming a different distribution of periods at least in those clusters where the efficiency of the ionization process is small. Unfortunately, the shape of this distribution is still largely uncertain (Halbwachs et al. 2003). Studies performed on large samples of binaries in the Galactic field are not able to distinguish between the various proposed distributions, suffering strong observational biases (Abt 1983; Eggleton, Tout & Fitchett 1989; Duquennoy & Mayor 1991; Halbwachs et al. 2003). Moreover, detections of long-period binary systems (with $P > 10^6$ d) are limited by the intrinsic impossibility to detect photometric and/or kinematical variability over such large time-scales. Given the importance of this parameter, an indication of the true shape of the period distribution would be valuable.

The predicted radial distribution of binary systems shows a decreasing trend with central peak and a rapid drop toward the external regions of the cluster. The reason at the basis of this behaviour is linked to the process of mass segregation which produces a concentration of the massive binary systems in the central region of the cluster. The higher concentration of binary systems has been already observed by several authors in different clusters (Yan & Reid 1996; Rubenstein & Bailyn 1997; Albrow et al. 2001; Bellazzini et al. 2002; Zhao & Bailyn 2005; Sollima et al. 2007).

The results of the code presented here have been compared with the most recent N -body and Monte Carlo simulations available in the literature. Despite the many adopted simplifications, the predictions of the code appear to be qualitatively consistent with the results of the above approaches. I estimated that at least an half of the difference between the fractions of survived binaries predicted by the N -body simulations by Hurley et al. (2007) and the Monte Carlo simulations by Ivanova et al. (2005) is due to the different assumptions made by these authors regarding the upper end of the periods distribution and the treatment of evaporation. The remaining difference can be addressed to the different initial cluster conditions assumed by these authors (as already suggested by Fregeau 2007).

The code presented here has been used to interpret the differences in the binary fractions measured in the sample of globular clusters presented by Sollima et al. (2007). There is no combination of initial parameters able to reproduce the observed fraction of binaries observed in group of clusters with different ages unless assuming a different initial binary content. The group of young globular clusters in the sample of Sollima et al. (2007) is formed by three clusters (viz. Terzan 7, Palomar 12 and Arp 2). These clusters are also the most distant from the Sun and they are thought to belong to the Sagittarius Stream (Bellazzini, Ferraro & Ibata 2003). Thus, they might be stellar systems with intrinsically different origins and properties, whose initial conditions could significant differ from those of 'genuine' Galactic globular clusters (see also Sollima et al. 2008). Future studies addressed to the estimate of the binary fraction in other clusters suspected to have an extragalactic origin will help to understand how the environmental conditions influence the original content of binaries of globular clusters.

ACKNOWLEDGMENTS

This research was supported by the Instituto de Astrofísica de Canarias. I warmly thank Antonino Milone and Natasha Ivanova for providing their preliminary results. I also thank the anonymous referee for his helpful comments and suggestions.

REFERENCES

- Abt H. A., 1983, *ARA&A*, 21, 343
 Albrow M. D., Gilliland R. L., Brown T. M., Edmonds P. D., Guhathakurta P., Sarajedini A., 2001, *ApJ*, 559, 1060
 Bailyn C. D., 1995, *ARA&A*, 33, 133
 Belczynski K., Kalogera V., Bulik T., 2002, *ApJ*, 572, 407
 Bellazzini M., 1998, *New Astron.*, 3, 219
 Bellazzini M., Fusi Pecci F., Messineo M., Monaco L., Rood R. T., 2002, *AJ*, 123, 509
 Bellazzini M., Ferraro F. R., Ibata R., 2003, *AJ*, 125, 188
 Bica E., Bonatto C., 2005, *A&A*, 431, 943
 Binney J., Tremaine S., 1987, *Galactic Dynamics*. Princeton Univ. Press, Princeton, NJ
 Bolte C. D., 1992, *ApJS*, 82, 145
 Clark G. W., 1975, *ApJ*, 199, L143
 Clark L. L., Sandquist E. L., Bolte M., 2004, *AJ*, 138, 3019
 Davies M. B., 1995, *MNRAS*, 276, 887
 Davies M. B., 1997, *MNRAS*, 288, 117
 Davies M. B., Benz W., 1995, *MNRAS*, 276, 876
 Di Stefano R., Rappaport S., 1994, *ApJ*, 437, 733
 Djorgovski S., 1993, in Djorgovski S. G., Meylan G., eds, *ASP Conf. Ser. Vol. 50, Structure and Dynamics of Globular Clusters*. Astron. Soc. Pac., San Francisco, p. 373
 Djorgovski S., Meylan G., 1993, *BAAS*, 25, 885
 Djorgovski S., Piotto G., Capaccioli M., 1993, *AJ*, 105, 6
 Duquennoy A., Mayor M., 1991, *A&A*, 248, 485
 Eggleton P. P., Tout C. A., Fitchett M. J., 1989, *ApJ*, 347, 998
 Fregeau J. M., 2007, in Vesperini E., Giersz M., Sills A. L., eds, *Proc. IAU Symp. 246, Dynamical Evolution of Dense Stellar Systems*. Cambridge Univ. Press, Cambridge, p. 239
 Fregeau J. M., Gürkan M. A., Joshi K. J., Rasio F. A., 2003, *ApJ*, 593, 772
 Fregeau J. M., Cheung P., Portegies Zwart S. F., Rasio F. A., 2004, *MNRAS*, 352, 1
 Gao B., Goodman J., Cohn H., Murphy B., 1991, *ApJ*, 370, 567
 Gnedin O. Y., Ostriker J. P., 1997, *ApJ*, 474, 223
 Gunn J. E., Griffin R. F., 1979, *AJ*, 84, 752
 Halbwachs J. L., Mayor M., Udry S., Arenou F., 2003, *A&A*, 397, 159
 Heggie D. C., 1975, *MNRAS*, 173, 729
 Heggie D. C., Hut P., McMillan S. L. W., 1996, *ApJ*, 467, 359
 Hills J. G., 1975, *AJ*, 80, 1075
 Hills J. G., 1992, *AJ*, 103, 1955
 Hills J. G., Day C. A., 1976, *Astrophys. Lett.*, 17, 87
 Hurley J. R., Shara M. M., 2003, *ApJ*, 589, 179
 Hurley J. R., Aarseth S. J., Shara M. M., 2007, *ApJ*, 665, 707
 Hut P. et al., 1992a, *PASP*, 104, 981
 Hut P., McMillan S., Romani R. W., 1992b, *ApJ*, 389, 527
 Ivanova N., 2006, *ApJ*, 636, 979
 Ivanova N., Belczynski K., Fregeau J. M., Rasio F. A., 2005, *MNRAS*, 358, 572
 King I. R., 1966, *AJ*, 71, 64
 Kim E., Yoon I., Lee H. M., Spurzem R., 2008, *MNRAS*, 383, 2
 Kim S. S., Lee H. M., 1999, *A&A*, 347, 123
 Kroupa P., 2002, *Sci*, 295, 82
 Lee H. M., Nelson L. A., 1988, *ApJ*, 334, 688
 Lee H. M., Ostriker J. P., 1986, *ApJ*, 310, 176
 McClure R. et al., 1986, *ApJ*, 307, L49
 McCrea W. H., 1964, *MNRAS*, 128, 147
 Michie R. W., 1963, *MNRAS*, 125, 127
 Mikkola S., 1983a, *MNRAS*, 203, 1107
 Mikkola S., 1983b, *MNRAS*, 205, 733
 Milone A., Piotto G., Bedin L. R., Sarajedini A., 2008, *Mem. Soc. Astron. Ital.*, preprint (arXiv:0801.3177)
 Pietrinferni A., Cassisi S., Salaris M., Castellì F., 2006, *ApJ*, 642, 797
 Piotto G. et al., 2004, *ApJ*, 604, L109
 Portegies Zwart S. F., Hut P., McMillan S. L. W., Verbunt F., 1997a, *A&A*, 328, 143
 Portegies Zwart S. F., Hut P., Verbunt F., 1997b, *A&A*, 328, 130

- Portegies Zwart S. F., McMillan S. L. W., Hut P., Makino J., 2001, *MNRAS*, 321, 199
- Rasio F. A., Pfahl E. D., Rappaport S., 2000, *ApJ*, 532, L47
- Romani R. W., Weinberg M. D., 1991, *ApJ*, 372, 487
- Rubenstein E. P., Bailyn C. D., 1997, *ApJ*, 474, 701
- Shara M. M., Hurley J. R., 2002, *ApJ*, 571, 830
- Sigurdsson S., Phinney E. S., 1995, *ApJS*, 99, 609
- Sills A. et al., 2003, *New Astron.*, 8, 605
- Smith K. W., Bonnell I. A., 2001, *MNRAS*, 322, L1
- Sollima A., Beccari G., Ferraro F. R., Fusi Pecci F., Sarajedini A., 2007, *MNRAS*, 380, 781
- Sollima A., Lanzoni B., Beccari G., Ferraro F. R., Fusi Pecci F., 2008, *A&A*, 481, 701
- Sweatman W. L., 2007, *MNRAS*, 377, 459
- Trager S. C., King I. R., Djorgovski S., 1995, *AJ*, 109, 218
- Trenti M., Heggie D. C., Hut P., 2007, *MNRAS*, 374, 344
- Weidemann V., 2000, *A&A*, 363, 647
- Yan L., Cohen J. G., 1996, *AJ*, 112, 1489
- Yan L., Mateo M., 1994, *AJ*, 108, 1810
- Yan L., Reid M., 1996, *MNRAS*, 279, 751
- Zhao B., Bailyn C. D., 2005, *AJ*, 129, 1934

APPENDIX A: PARTIALLY RELAXED MULTIMASS KING MODELS

The density and velocity distribution profiles of globular clusters are well represented by King models (King 1966). These models assume that cluster stars located at a distance r from the cluster centre follow a distribution of velocities

$$f(\epsilon, J) = Ae^{-\beta J^2} (e^{-\epsilon_r/K} - 1) \quad (\text{A1})$$

(Michie 1963; King 1966; Gunn & Griffin 1979).

Here K is a quantity proportional to σ_v^2 that accounts for the cluster relaxation, ϵ_r is the energy for unity of mass ($\epsilon_r = \Phi_r + v^2/2$), J

is the angular momentum and A is a normalization factor. The term $\exp(-\beta J^2)$ accounts for anisotropies in the distribution function (here I set this quantity equal to unity). The shape of distribution of stars in these models is completely defined by the King parameter $W_0 = -\Phi_0/\sigma_v^2$. The density profile can be derived from the above distribution considering the Poisson equation and the relation

$$\rho_r(m) = \int_0^{v_{e,r}} f(v, r) d^3v.$$

After a time-scale comparable to the local relaxation time, collisions become frequent and produce the equipartition of the kinetic energy ($K \propto m^{-1}$). Under this condition, the distribution of velocities becomes a function of the mass. Otherwise, the distribution of velocities does not depend on mass ($K = \text{constant}$) and the above formulation reduces to the case of a single-mass King model. However, relaxation occurs after different time-scales at different distances from the cluster centre (see equation 1). Therefore, only a fraction of stars follow relaxed orbits.

For this reason, the code calculates at each time-step of the simulation the fraction of stars located in the region where relaxation already occurred. Defining

$$\gamma = \frac{N_m(r < r_{\text{rel}})}{N_m}$$

the distribution of velocities has been then assumed to follow the form of equation (A1) where

$$K = \frac{\gamma \langle m \rangle + (1 - \gamma)m}{m} \sigma_v^2.$$

The density and velocity dispersion profiles have been therefore calculated accordingly.

This paper has been typeset from a $\text{\TeX}/\text{\LaTeX}$ file prepared by the author.